Ferrocenyl naphthalene diimides as tetraplex DNA binders

Shinobu Sato, Shigeori Takenaka *

Department of Applied Chemistry, Research Center for Biomicrosensing Technology, Kitakyushu 804-8550, Japan

ARTICLE INFO

ABSTRACT

Seven ferrocenyl naphthalene diimide (FND) ligands were synthesized. Each had a higher affinity for tetraplex DNA than for either single- or double-stranded DNA. The FND binding affinities were > 10^5 M^{-1} in 0.10 M AcOH-AcONa or AcOH-AcOK (pH 5.5) containing 0.10 M NaCl or KCl. The FNDs with the highest binding affinities for tetraplex DNA showed 23- or 8-times higher preference for tetraplex DNA than for single- or double-stranded DNA, respectively. The current signals generated from the seven FNDs bound to the tetraplex DNA immobilized on the electrode were found to correlate with the binding affinities of these ligands for the tetraplex DNA. Furthermore, using the telomerase repeat amplification protocol assay, the FND ligands could be categorized into three groups: (a) inhibiting both telomerase and Taq polymerase, (b) inhibiting telomerase alone, and (c) inhibiting neither telomerase nor Taq polymerase.

© 2016 Published by Elsevier Ltd.

1. Introduction

Telomerase, a ribonucleoprotein, is an enzyme that elongates telomeric DNA located at the termini of chromosomal DNA. Telomerase from cancer cells has been characterized and is expected to be a new cancer marker [1]. Telomerase activity is estimated by the telomerase repeat amplification protocol (TRAP) assay [2]. However, contaminants in the sample sometimes inhibit the polymerase chain reaction (PCR) in the TRAP assay, leading to erroneous results [3]. Therefore, an alternative method for the precise detection of telomerase activity is required.

Maesawa et al. [4] monitored the telomerase activity by using surface plasmon resonance (SPR) coupled with a telomerase substrate (TS)-primer-immobilized gold surface. An electrochemical method has been developed based on the TS-primer-immobilized electrode to obtain highly sensitive detection of telomerase [4–6,8,10–13]. Since the elongated TS-primer-immobilized electrode contains a TTAGGG repeating sequence, telomerase activity can be estimated by measuring the guanine oxidation current [5]. To further improve the sensitivity of the system, nanoparticles were attached to the elongated DNA and subsequently Ag was deposited to successfully measure telomerase activity from a single cell [6]. We used the hexaammonium ruthenium complex, which is known to bind to one molecule per three phosphate anions or three bases [7], to quantitate the elongated TS-primer-immobilized electrode [8]. This method has been used to estimate the telomerase activity of 5–1000 cells. These examples show that the TS-primer-immobilized electrode can be used for highly sensitive detection of telomerase activity, using a relatively simple method.

Naphthalene diimide derivatives are known to bind to the tetraplex structures found in human telomeric DNA [9–12]. Several kinds of ferrocenyl naphthalene diimides (FNDs), 1–7 (Fig. 1), have been developed as hybridization indicators [13]. Furthermore, we showed that 7 binds to tetraplex DNA with much higher affinity than it does to double-stranded DNA, and we applied 7 to the electrochemical telomerase assay (ECTA) [9]. In this assay, the TS-primer on the immobilized electrode was elongated depending on the telomerase activity in the sample, and the elongated DNA formed a tetraplex structure in an electrolyte containing KCl; 7 concentrated on the surface of this electrode by binding to the tetraplex DNA, resulting in an increased current signal. Telomerase activity of the extracts from 10 HeLa cells was detected by this ECTA [9]. Derivative 3, which has a lower redox potential than that of 7 [13], was applied to detect the telomerase activity, using ECTA, from the extracts of SAS, Ca9-22, HSC-2, and HSC-3 cultured cells, which originate from oral cancer [14]. Cancer diagnosis was successfully achieved from clinical samples of patients with oral cancer, using ECTA with derivative 3 [14–16]. Here, we analyzed the selectivity of 3 for single-stranded, double-stranded, and tetraplex DNA; the interaction of 1–7 with tetraplex DNA, and the inhibition ability of telomerase.

2. Experimental

2.1. Materials

FNDs 1–7 were synthesized according to the procedures described previously [9,13,17,18]. AcOK-AcOH and AcONa-AcOH buffers (pH 5.5) were prepared using potassium acetate (Wako, Tokyo, Japan), glacial acetic acid (Wako), and sodium acetate (Wako). Tris(hydroxymethyl)aminomethane (Tris)-HCl (pH 7.4) was purchased from Sigma-Aldrich. Hexaammonium ruthenium [Ru(NH$_3$)$_6$Cl$_3$] was pur-

* Corresponding author.
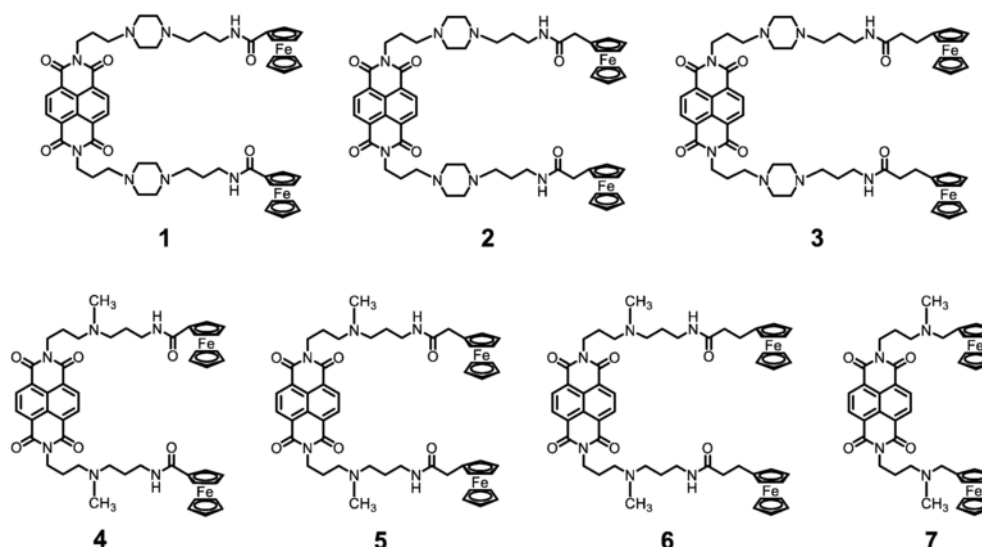Email address: shige@she.kyutech.ac.jp (S. Takenaka)

Fig. 1. Chemical structure of FND 1–7.

chased from Wako. The oligonucleotides used in this experiment were custom-synthesized from Genenet (Fukuoka, Japan) (Table 1). A-core, TA-core, and dsDNA (100 μM) were incubated with 0.10 M AcONa-AcOH (pH 5.5) containing 0.10 M NaCl or 0.10 M AcOK-AcOH (pH 5.5) containing 0.10 M KCl at 95 °C for 10 min and cooled slowly over 2 h. Tetraplex DNA were kept at 4 °C before use.

2.2. UV–Vis measurements

A small portion of the 100-μM TA-core in 0.10 M AcONa-AcOH (pH 5.5) containing 0.10 M NaCl was added to 3.0 μM 3 in 0.10 M AcONa-AcOH (pH 5.5) containing 0.10 M NaCl, and their absorption spectrum change was monitored. Absorption titration of 7 was also carried out under these conditions. The absorption titrations of 3 and 7 were also carried out in 0.10 M AcOK-AcOH (pH 5.5) containing 0.10 M KCl. The observed spectrum changes at 384 nm were rearranged with Scatchard plot [19] as the following equation in the case of non-cooperative binding.

$$v/L = K\,(n - v) \tag{1}$$

where v, L, n, and K refer to the saturation fraction as the amount of bound ligand per added DNA, amount of unbound ligand, bonding number of ligand per one DNA molecule, and binding affinity, respectively. The K and n values were obtained from Eq. (1), calculated using the v and L in the different ratio of ligand and DNA concentration obtained using the non-linear least-squares method.

Table 1
DNA sequence used in this experiment.

Abbreviation	Sequence
ssDNA	5′-GCG AAA CCT CCC-3′
dsDNA	5′-GCG AAA CCT CCC-3′
	3′-CGC TTT GGA GGG-5′
TA-core	5′-TAG GGT TAG GGT TAG GGT TAG GG-3′
TS	HO-(CH$_2$)$_6$-S-S-(CH$_2$)$_6$–5′-AAT CCG TCG AGC AGA GTT-3′
TS4	HO-(CH$_2$)$_6$-S-S-(CH$_2$)$_6$–5′-AAT CCG TCG AGC AGA GTT AGG GTT AGG GTT AGG GTT AGG G-3′

2.3. Isothermal titration calorimetry (ITC)

TA-cores (10 μM or 50 μM) in 0.10 M AcOK-AcOH (pH 5.5) containing 0.10 M KCl or AcONa-AcOH containing 0.10 M NaCl were heated at 95 °C for 10 min and subsequently cooled to 25 °C at 1.0 °C/min before being used for ITC. Binding studies were performed using low volume Nano ITC (TA instruments, USA), with a cell volume of 170 μL, at 30 °C. All solutions were dissolved in 0.10 M AcOK-AcOH (pH 5.5) containing 0.10 M KCl or AcONa-AcOH containing 0.10 M NaCl and were degassed for 10 min before use. For 1, 2, or 4–7, the sample cell was filled with the 10 μM TA-core, and 3 μL of 150 μM 1, 2, 4, 5, 6, or 7 was added into the thermostated cell repeatedly using a syringe. However, for 3, the sample cell was filled with 10 μM 3, and 3 μL of the 50-μM TA-core was added into the thermostated cell repeatedly using a syringe. This reverse titration was carried out to avoid the occurrence of aggregation, which could result from titrating excess TA-core with a small portion of 3.

2.4. Circular dichroism (CD)

CD spectra of the 1.5 μM TA-core were measured in 0.10 M AcOK-AcOH (pH 5.5) containing 0.10 M KCl or AcONa-AcOH containing 0.10 M NaCl at 25 °C, in the absence or presence of 1.5, 3.0, or 4.5 μM of 1–7, at a scan rate of 50 nm/min, using a Jasco J-820 spectropolarimeter (Tokyo, Japan) with the following conditions: response, 2 s; data interval, 0.1 nm; sensitivity, 100 mdeg; bandwidth, 2 nm; and scan number, 4 times.

Melting curves of the 1.5-μM TA-core at 292.6 nm or 295 nm were measured in 0.10 M AcOK-AcOH (pH 5.5) containing 0.10 M KCl or AcONa-AcOH containing 0.10 M NaCl, in the absence or presence of 4.5 μM of 1–7, using a Jasco J-820 spectrophotometer equipped with a temperature controller with the following conditions: response, 100 mdeg; temperature gradient, 60 °C/h; response, 8 s; data collecting interval, 0.5 °C; and bandwidth, 2 nm. Three milliliters of total volume was used in the cell with 1 cm of light path length.

2.5. TRAP assay

A TRAP assay was performed using a TRAPeze kit (EMD Millipore) according to the manufacturer's instructions. Lysate protein was treated using the TRAPese kit's positive-control cell according to the manufacturer's instructions. The telomerase reaction solution (50 μL) consisted of 20 mM Tris–HCl, pH 8.3; 1.5 mM MgCl$_2$; 63 mM KCl; 0.05% Tween 20; 1.0 mM ethyleneglycol-bis(β-aminoethyl)-N,N,N',N'-tetraacetic acid; 50 μM each dNTP mixture; 1 × TS primer; 1 × primer mix; 2.0 units of Taq polymerase; 250 cells of the lysate protein; and 0, 0.5, 1.0, 10, 25, 50 μM **1**–**7**. Reactions were run under the following conditions: 1 × 30 °C, 1 h; 33 × (95 °C, 30 s, 59 °C, 1 min, 72 °C, 30 s); 1 × 72 °C, 20 min. Gel electrophoresis on 12.5% polyacrylamide prepared in 1.25 × TBE (89 mM Tris base, 89 mM borate, and 1 mM ethylenediaminetetraacetic acid, pH 8.0) was run at 200 V for 1 h in 0.7 × TBE. After electrophoresis, the gel was stained with 1 × GelStar® Nucleic Acid Stain in 1 × TBE for 30 min and photographed.

2.6. Preparation of TS- or TS4-immobilized electrode

Gold electrode (φ = 1.6 mm, BAS Inc., Tokyo, Japan) was mechanically polished with 0.05 μm alumina slurry for 60 min and sonicated in Milli-Q water thrice for 5 min. The potential was set as a reference against Ag/AgCl. This electrode was measured by Cyclic Voltammetry (CV), with 2 V/s and 500 segments × 6 times (from − 0.35 to − 1.35 V) in 0.50 M NaOH; it was washed with Milli-Q water [20] and subsequently treated with Multi Potential Step (1st step: 2 V for 5 s and 2nd step: − 0.35 V for 10 s) in 0.50 M H$_2$SO$_4$. CV was then measured with 4 V/s and 40 segments (from − 0.35 to 1.5 V), after which the electrode was washed with Milli-Q water. As the final step, CV was measured with 0.1 V/s and 4 segments (from − 0.35 to 1.5 V), after which the electrode was washed with Milli-Q water. The oxidation peak area at 0.9 V was calculated in the CV [21]. Electrodes were dipped into 95 μl solution containing 10 nM TS or 10 nM TS4 with 50 mM NaCl in 2 ml microtubes and incubated at 37 °C for 16 h. After washing with Milli-Q water and removing the water droplets, the electrode was dipped into 80 μl of 1 mM mercaptohexanol in a 2-ml microtube and incubated at 45 °C for 1 h, after which it was washed again with Milli-Q water.

2.7. Chronocoulometry (CC)

CC measurement was carried out in three electrodes with Ag/AgCl as a reference electrode system, Pt wire as a counter electrode, and the DNA immobilized electrode as a working electrode, using Electrochemical Analyzer Model 630A (CH Instruments, TX). A TS- or TS4-immobilized electrode was used for CC measurement in 10 mM Tris–HCl (pH 7.4) at 25 °C. After washing with Milli-Q water, CC measurement of the electrode was carried out in 10 mM Tris–HCl (pH 7.4) containing 50 μM Ru (NH$_3$)$_6$Cl$_3$ at 25 °C. CC measurement was carried out under the following conditions: initial voltage, 0.1 V; final voltage, − 0.4 V; Step 1, pulse width: 0.25 s, sample interval: 0.25 ms, quiet time: 2 s, and sensitivity: 1 × 10$^{−5}$ A/V. The amount of DNA on the electrode was estimated using the method by Tarlov and co-workers [7].

2.8. Differential pulse voltammetry (DPV)

DPV of the TS- or TS4-immobilized electrode was carried out in 0.10 M AcOK-AcOH (pH 5.5) and 0.10 M KCl containing 20 μM **1**–**7** at 25 °C. The DPV measurement conditions were as follows: initial voltage, 0 V; final voltage, 0.7 V; potential increase, 0.02 V; amplitude, 0.05 V; pulse width, 0.05 s; sampling width, 0.02 s; pulse period, 0.2 s; quiet time, 2 s; and sensitivity, 1 × 10$^{−6}$ A/V.

3. Results and discussion

3.1. Binding behaviors of **1**–**7** with TA-core

Thermodynamic parameters of the interaction between **1** and **7** and the TA-core, which is known as a hybrid-type G-quartet structure [22], were measured by the ITC titration of 150 μM **1**–**7** with the 10-μM TA-core in 0.10 M AcONa-AcOH (pH 5.5) containing 0.10 M NaCl or AcOK-AcOH containing 0.10 M KCl at 30 °C (Table 2, Figs. S1, S2). A small portion of 150 μM **1**–**7** in 0.10 M AcONa-AcOH (pH 5.5) containing 0.10 M NaCl or AcOK-AcOH containing 0.10 M KCl was added to the same buffer containing the 10 μM TA-core. Stable thermal changes were observed in **1**, **2**, **4**–**7**, whereas unstable thermal changes were observed in **3**. This could be due to **3**'s low solubility to induce aggregation in the cell. Therefore, thermodynamic parameters were obtained by reverse titration carried out using 10 μM **3**: the ITC titration of the 10-μM TA-core with 10 μM **3** in 0.10 M AcONa-AcOH (pH 5.5) containing 0.10 M NaCl or AcOK-AcOH containing 0.10 M KCl.

The binding ratios of these ligands to tetraplex DNA were all 2:1, except for **1** and **3** in the presence of NaCl. The 2:1 ratio suggested a stacking of the ligands to the upper and lower G-quartet aromatic planes. We have previously shown that **1**, **2**, **4**, **5**, and **7** have intermolecular stacking structures between naphthalene diimide and the ferrocene planes, whereas **3** and **6** have non-stacking structures in aque-

Table 2
Binding parameter of **1**–**7** with TA-core under NaCl or KCl by ITC measurements.

		1	2	3[a]	4	5	6	7
NaCl[1)	$10^{−5}$ K/M$^{−1}$	4.55	2.17	86.9	7.59	7.59	61.2	5.71
	n	3	2	3	2	2	2	2
	ΔH/kcal mol$^{−1}$	− 2.92	− 7.92	− 15.7	− 5.04	− 5.07	− 4.40	− 4.11
	TΔS/cal mol$^{−1}$	4.93	− 0.52	− 6.11	3.12	3.09	5.02	3.88
	ΔG/kcal mol$^{−1}$	− 7.85	− 7.40	− 9.63	− 8.16	− 8.16	− 9.42	− 7.99
KCl[2)	$10^{−5}$ K/M$^{−1}$	9.75	6.16	57.3	7.52	8.34	27.9	9.99
	n	3	2	2	2	2	2	2
	ΔH/kcal mol$^{−1}$	− 3.74	− 7.60	− 9.40	− 3.57	− 6.91	− 5.11	− 3.72
	TΔS/cal mol$^{−1}$	4.57	0.43	− 0.03	4.58	1.30	3.83	4.60
	ΔG/kcal mol$^{−1}$	− 8.31	− 8.03	− 9.37	− 8.15	− 8.21	− 8.94	− 8.32

1) 0.10 M AcONa-AcOH(pH 5.5), 0.10 M NaCl, 30 °C.
2) 0.10 M AcOK-AcOH(pH 5.5), 0.10 M KCl, 30 °C.

[a] Reverse titration was carried out to avoid to aggregation.

ous solution [13]. This suggests that these ligands bind to the tetraplex structure through the stacking between naphthalene diimide and the G-quartet planes and that the binding behavior of these ligands is correlated with their initial conformations: an intramolecular-stacked ligand has to be broke before stacking with G-quartet planes of tetraplex DNA.

The ΔH and T·ΔS values in the binding process of these derivatives with a TA-core were −2.9 to −7.9 kcal mol^{-1} and 0.5 to −5.0 kcal mol^{-1}, respectively. For **2** and **3**, a large contribution of enthalpy and little or no contribution of entropy were obtained, which suggested the stable complex formation of **2** and **3** through the additional interaction of their linker chains such as hydrogen bonding. These derivatives, except **2** and **3**, showed similar contributions of enthalpy and entropy, and these cases might show effective contribution of the π-π-stacking interaction and dehydration after complex formation. Given that these data are similar to previous reports for H$_2$TMPyP [23], anthracene derivative [24], Phen-DC3 [25], and 360A-Br [25] as tetraplex binders, it is suggested that the main force in this binding process contributes to the similar mechanism of π-π-stacking.

Thermal stability of G-quadruplex with binding of **1–7** was evaluated with Tm measurement (Table 3, Fig. S3). The Tm values of TA-core increased 1.5–6.0 °C in the presence of these derivatives, with **3** and **6** showing the highest stabilization values, which is in agreement with the results of the binding analysis. CD spectra of TA-core upon addition of **1–7** were measured to obtain their detailed tetraplex structure. A TA-core has a basket-type tetraplex structure in 0.10 M AcONa-AcOH (pH 5.5) containing 0.10 M NaCl, with positive bands at 295 nm and 245 nm and a negative band at 268 nm (Fig. S4). The positive band at 295 nm was slightly increased, with almost no change of the other bands, upon addition of 1.5, 3.0, and 4.5 μM of **1–7** (Fig. S4). CD spectra of TA-cores, measured in 0.10 M AcOK-AcOH (pH 5.5) containing 0.10 M KCl (Fig. S5), showed hybrid-type tetraplex structures based on a positive band at 290 nm, a shoulder at 270 nm, and a negative band at 240 nm. Interestingly, the shoulder at 270 nm and the shift with longer wavelength at 290 nm disappeared in **1–3** carrying piperazine linkers, whereas for **4–7** the shoulder was only decreased. These results show that **1–3** induced the anti-parallel structure from a hybrid one after their binding, and **4–7** bind to the tetraplex structure without dramatic structural changes.

Table 3
Tm values of TA-core with **1–7** under NaCl or KCl.

| | Tm/°C | | | | | | | |
	TA-core	+ **1**	+ **2**	+ **3**	+ **4**	+ **5**	+ **6**	+ **7**
NaCl	52	54	54	56	54	54	58	56
KCl	68	71	69	72	71	71	72	72

3.2. Binding affinity of **3** with single-stranded, double-stranded, and tetraplex DNA

The above results show that **3** and **6** have higher binding affinities for tetraplex DNA than **1**, **2**, **4**, **5**, **7** do. To evaluate the performance of **3** and **7** for single-stranded, double-stranded, and tetraplex DNA, the binding behaviors of **3** and **7** were compared using Scatchard analysis.

Table 1 shows the 12-mer DNA sequences used in this experiment. Changes in the absorption spectra of 6.0 μM **3** and **7** in 0.10 M AcONa-AcOH containing 0.10 M NaCl were measured upon addition of 150 μM ssDNA, 100 μM dsDNA, or 100 μM TA-core. Addition of the three kinds of DNA showed large hypochromic and small red shifts with isosbestic point, resulting in single mode binding of **3** and **7** to these DNAs. The binding constant (K) and binding number (n) were calculated with Scatchard analysis using the absorption changes of **3** and **7** at 384 nm upon addition of DNA (Table 4, Fig. S6). The binding affinity of **3** with tetraplex, double-stranded, or single-stranded DNA was 2.3 × 10^7, 2.8 × 10^6, or 9.9 × 10^5 M^{-1}, respectively; the binding affinity of **7** was 2.6 × 10^6, 9.9 × 10^5, or 1.3 × 10^5 M^{-1}, respectively. The binding affinity of **7** for tetraplex DNA was 20- and 3-times higher than its binding affinity for single- and double-stranded DNA, respectively. The binding affinity of **3** for tetraplex DNA was similar to that for single-stranded DNA, but was 8-times higher than that for double-stranded DNA. The binding numbers of **3** per 12-mer single-stranded, double-stranded, and tetraplex DNA were 4, 6, and 3, respectively. Four molecules of **3** bound to the 12-meric single-stranded DNA with electrostatic interaction or stacking between naphthalene diimide and the nucleic bases. Six molecules of **3** bound to the double-stranded 12-meric DNA, which can be explained by considering that every two base pairs were bound based on the neighbor-exclusion principle of DNA intercalation [18]. Three molecules of **3** bound to tetraplex DNA, suggesting that two or one of **3** was stacked in the upper or lower G-quartet planes, which is similar to the result of previously reported tetraplex binders [26].

3.3. Evaluation of telomerase inhibition of **1–7** in the TRAP assay

A TRAP assay was performed using 250 cell lysates with varying amounts of **1–7** to evaluate their telomerase inhibition ability. Gel electrophoresis results of the TRAP assay in the presence of 0.5–50 μM **7** are shown in Fig. 3, where the lowest band and bands every 6-bp were observed as an internal control of Taq polymerase of PCR and telomerase, respectively, at least in the case of ligand concentrations lower than 0.1 μM. This result showed that **7** did not inhibit telomerase or Taq polymerase as shown in Fig. 2 and Table 5. The bands at every 6-bp were not observed for **1–3** under 0.5–50 μM in the TRAP assay. This result shows that **1–3** inhibit telomerase activity without inhibiting Taq polymerase. On the other hand, the every 6-bp bands dis-
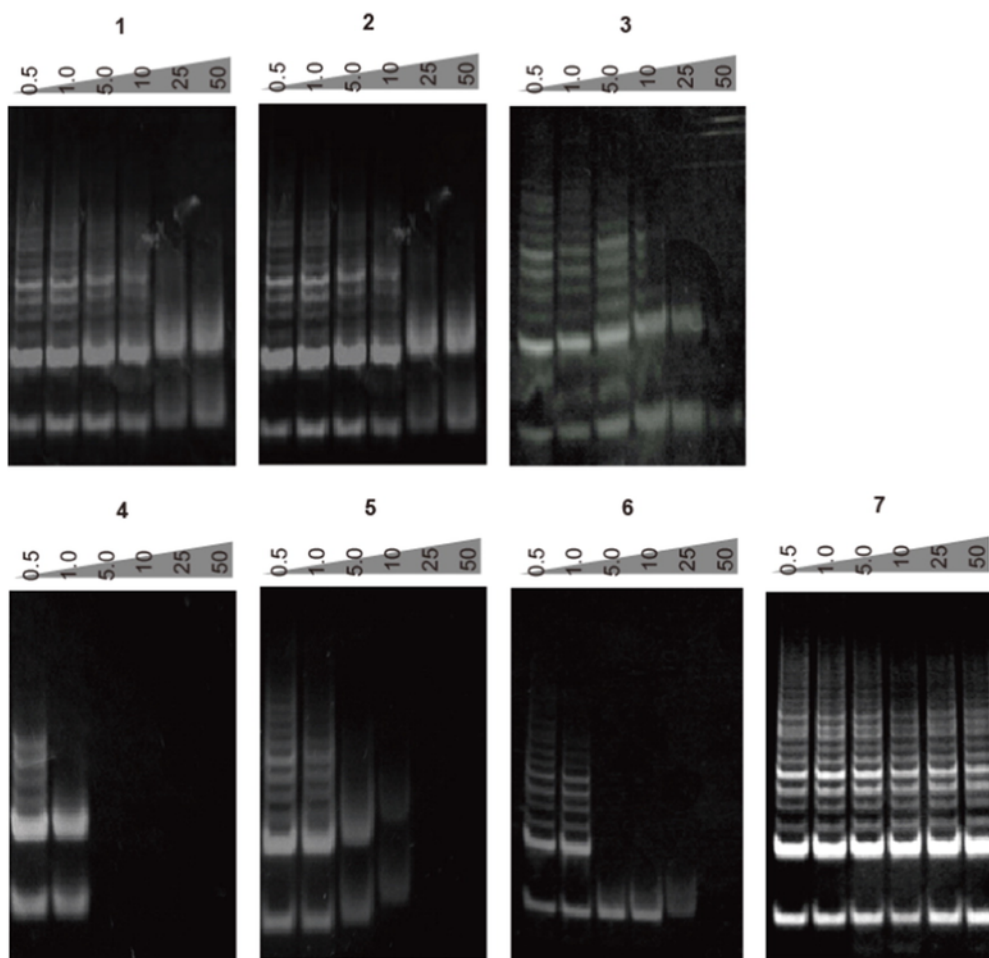
Table 4
Binding affinity and Binding number of **3** or **7** with A-core under NaCl or KCl obtained from Scatchard analysis.

| | **3** | | | | **7** | | | |
| | 10^{-5} K/M^{-1} | n | Selectivity | | 10^{-5} K/M^{-1} | n | Selectivity | |
			vs. ssDNA	vs. dsDNA			vs. ssDNA	vs. dsDNA
ssDNA[a]	9.9	4			1.3	5		
dsDNA[a]	28	6	3		9.9	7	8	
TA-core (NaCl)[a]	230	3	23	8	26	3	20	3
TA-core (KCl)[b]	110	3	11	4	36	3	28	4

[a] 0.10 M AcONa-AcOH(pH 5.5), 0.10 M NaCl, 25 °C.
[b] 0.10 M AcOK-AcOH(pH 5.5), 0.10 M KCl, 25 °C.

Fig. 2. Gel electropherogram of TRAP assay in the presence of the varied amount of **1**–**7**.

Table 5
Inhibition concentration of Telomerase and Taq polymerase.

	1	2	3	4	5	6	7
Telomerase	25 μM	25 μM	25 μM	1.0 μM	5.0 μM	5.0 μM	–
Taq polymerase	–	–	–	5.0 μM	25 μM	50 μM	–

appeared at concentrations of 1.0 μM in **4**, 5.0 μM in **5**, and 5.0 μM in **6**, and all the telomerase and Taq polymerase based bands disappeared at concentrations of 5.0 μM in **4**, 25 μM in **5**, and 50 μM in **6**, with 250 cell lysate. The inhibitory ability of these derivatives might be correlated with their affinity for tetraplex DNA, because of no correlation between their affinities for double stranded DNA and the control gel band to check PCR progress (Table S1). Derivatives **4**–**6**, carrying the same linker chain, seem to bind in a hybrid-type tetraplex DNA structure maintained from the initial CD titration experiments (Fig. S5, E-F). Tm values for the hybrid-type tetraplex structure are higher than those for the basket-type one. Because the complex with the hybrid-type tetraplex structure was more stable than that with the basket-type one under the TRAP assay condition of 59–95 °C, these derivatives, which stabilize the complex with tetraplex DNA structure, exhibit higher inhibitory ability for telomerase.

3.4. Electrochemical behaviors of 1–7

A TS-primer (TS) and a TS-primer attached to (TTAGGG)$_4$ (TS4)-immobilized on the electrode were prepared. The immobilization densities of these electrodes (Γ_{TS}, Γ_{TS4}) were estimated with CC measurement using the hexamine ruthenium complex. SWV of two electrodes (i_{TS}, i_{TS4}) were measured in 0.10 M AcOK-AcOH containing 0.10 M KCl and 20 μM **1**–**7**, and oxidation currents I_{NTS} ($= i_{TS}/\Gamma_{TS}$) and I_{NTS4} ($= i_{TS4}/\Gamma_{TS4}$) per single DNA molecule were estimated (Figs. S8, S9). Circular dichromic spectra of TS4 showed a positive band at 290 nm and a negative band at 240 nm under 0.10 M AcOK-AcOH containing 0.10 M KCl (Fig. S7), suggesting its tetraplex structure formation (anti parallel structure), under the same conditions as those for SWV measurement. Since the density of immobilized DNA on each individual electrode will differ, SWV current I_N was normalized per immobilized DNA molecule electrode measured by CC. The results show that the SWV current for the tetraplex DNA I_{NTS4} correlated with the Kn obtained from the ITC measurements; the ligand carrying higher binding constant and binding number showed higher current (Fig. 3).

Since the electrolyte contained 20 μM of these derivatives, which was more than the amount of DNA on the electrode, the DNA was saturated with ligands. However, the binding numbers of these derivatives with tetraplex DNA differed, due to the binding constant and binding number for the individual derivative, and therefore the obtained
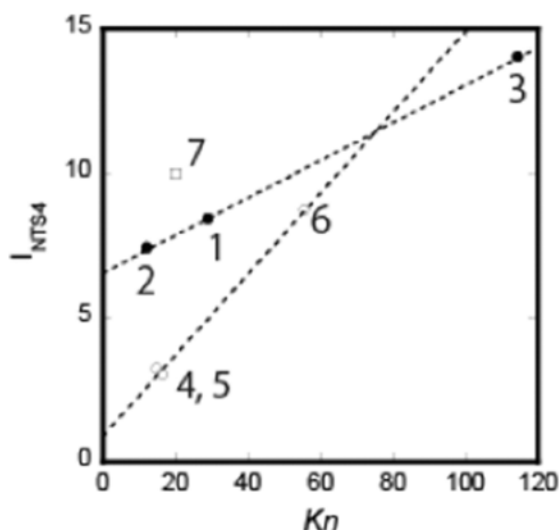
Fig. 3. Correlation between Kn values and I_{NTS4} in 0.10 M AcOK-AcOH containing 0.10 M KCl.

data were arranged by $n \times K$ value. When observed more closely, **1–3**, **4–6**, and **7** show different behaviors, which might come from the induced structure of tetraplex DNA bound with **1–3** and **4–6** by CD titration measurements. It is known that the different structures were induced by the different flexibilities of DNA on the electrode [27,28], leading to the different electrochemical behaviors observed.

Since the SWV peak for these ligands differs in the TS-immobilized electrode, selectivity of tetraplex DNA to single-stranded DNA was calculated as I_{NTS4}/I_{NTS} (Table 6). TS has an 18-mer single-stranded DNA and TS4 has a 24-mer tetraplex DNA with a 16-mer single-stranded DNA. If FND bound to TS and TS4 only with an electrostatic interaction, the current of TS4 (I_{NTS4}) should have been twice that of TS (I_{NTS}). Ligand **2** shows higher binding for single-stranded DNA. More than two-fold current increases were observed for **1**, **3**, **5**, and **6**, which show that these ligands are tetraplex-specific, exhibiting higher binding affinity based on ITC measurement. In other words, higher current shift was observed for the ligand carrying higher affinity for tetraplex DNA. Ligand **3**, which has the highest affinity for tetraplex DNA, was the most effective ligand in this system.

4. Conclusion

Binding constants of **1–7** with tetraplex DNA were $> 10^5$ M^{-1}, showing high preference for tetraplex DNA. The inhibition ability of telomerase and Taq polymerase differed amongst the derivatives,

Table 6
Electrochemical properties of TS- or TS4-immobilized electrode.

Parameter	FND						
	1	2	3	4	5	6	7
$10^{-11}\Gamma_{TS}$ (molecules/cm^2)	1.89	1.20	2.07	3.94	2.74	3.18	1.55
$10^{-11}\Gamma_{TS4}$ (molecules/cm^2)	0.73	1.24	0.68	1.97	1.28	1.15	0.91
$10^{-6}\, i_{TS}$ (A/cm^2)	6.2	7.4	8.7	6.5	3.5	13	8.0
$10^{-6}\, i_{TS4}$ (A/cm^2)	6.1	9.2	9.3	6.4	3.8	10	9.1
$10^{-16}\, I_{NTS}$ (A/molecules)	3.3	6.2	4.2	1.7	1.3	4.0	5.2
$10^{-16}\, I_{NTS4}$ (A/molecules)	8.4	7.4	14	3.2	3.0	8.7	10
I_{NTS4}/I_{NTS}	2.5	1.2	3.3	1.9	2.3	2.2	2.0

which provided important insight into the interaction of ligand with tetraplex DNA. Under an electrochemical response using single-stranded and tetraplex DNA-immobilized electrodes, the current response of tetraplex DNA to single-stranded DNA was highest in **3**. Using ECTA coupled with **3** for diagnosis of clinical samples showed > 80% sensitivity and specificity, which was consistent with our previous results [15,16].

Acknowledgements

Appendix A. Supplementary data

Supplementary data to this article can be found online at doi:10.1016/j.jinorgbio.2016.11.020.

References

[1] E. Hiyama, K. Hiyama Cancer, Letters 194 (2003) 221–233.
[2] N.W. Kim, et al., Science 266 (1994) 2011–2015.
[3] H. Yaku, T. Murashima, D. Miyoshi, N. Sugimoto, Molecules 18 (2013) 11751–11767.
[4] C. Maesawa, et al., Nucleic Acids Res. 31 (2003), e4.
[5] U. Eskiocak, D. Ozkan-Ariksoysal, M. Ozsoz, H.A. Oktem, Anal. Chem. 79 (2007) 8807–8811.
[6] L. Wu, J. Wang, J. Ren, X. Qu, Adv. Funct. Mater. 24 (2014) 2727–2733.
[7] A.B. Steel, T.M. Herne, M.J. Tarlov, Anal. Chem. 70 (1998) 4670–4677.
[8] S. Sato, S. Takenaka, Anal. Chem. 84 (2012) 1772–1775.
[9] S. Sato, H. Kondo, T. Nojima, S. Takenaka, Anal. Chem. 77 (2005) 7304–7309.
[10] I. Czerwinska, S. Sato, S. Takenaka, Bioorg. Med. Chem. 20 (2012) 6416–6422.
[11] Y. Esaki, Md. M. Islam, S. Fujii, S. Sato S. Takenaka, Chem. Commun. 50 (2014) 5967–5969.
[12] F. Cuenca, O. Greciano, M. Gunaratnam, S. Haider, D. Munnur, R. Nanjunda, W.D. Wilson, S. Neidle, Bioorg. Med. Chem. Lett. 18 (2008) 1668–1673.
[13] S. Sato, S. Takenaka, J. Organomet. Chem. 693 (2008) 1177–1185.
[14] K. Mori, S. Sato, M. Kodama, M. Habu, O. Takahashi, T. Nishihara, K. Tominaga, S. Takenaka, Clin. Chem. 59 (2013) 289–295.
[15] M. Hayakawa, S. Sato, I. Diala, M. Kodama, K. Tomoeda-Mori, K. Haraguchi, K. Tominaga, S. Takenaka, Electroanalysis 28 (2016) 503–507.
[16] M. Hayakawa, M. Kodama, S. Sato, K. Tomoeda-Mori, K. Haraguchi, M. Habu, S. Takenaka, K. Tominaga, Br. J. Oral Maxillofac. Surg. 54 (2016) 301–305.
[17] S. Sato, T. Nojima, M. Waki, S. Takenaka, Molecules 10 (2005) 693–707.
[18] S. Takenaka, K. Yamashita, M. Takagi, Y. Uto, H. Kondo, Anal. Chem. 72 (2000) 1334–1341.
[19] J.D. McGhee, von Hippel, J. Mol. Biol. 86 (1974) 469–489.
[20] Y. Xiao, R.Y. Lai, K.W. Plaxco, Nat. Protoc. 2 (2007) 2875–2880.
[21] S. Trastti, O.A. Petrii, Pure Appl. Chem. 63 (1991) 711–734.
[22] Z. Zhang, J. Dai, E. Veliath, R.A. Jones, D. Yang, Nucleic Acids Res. 38 (2010) 1009–1021.
[23] I. Haq, J.O. Trent, B.Z. Chowdhry, T.C. Jenkins, J. Am. Chem. Soc. 121 (1999) 1768–1779.
[24] P.J. Perry, A.P. Reszka, A.A. Wood, M.A. Read, S.M. Gowan, H.S. Dosanjh, J.O. Trent, T.C. Jenkins, L.R. Kelland, S. Neidle, J. Med. Chem. 41 (1998) 4873–4884.
[25] M. Boncina, C. Podlipnik, I. Piantanida, J. Eilmes, M.-P. Teulade Fichou, G. Vesnaver, J. Lah, Nucleic Acids Res. 43 (2015) 10376–10386.
[26] G.N. Parkinson, F. Cuenca, S. Neidle, J. Mol. Biol. 381 (2008) 1145–1156.
[27] A.-E. Radi, J.L.A. Sanchez, E. Baldrich, C.K. Osullivan, J. Am. Chem. Soc. 128 (2006) 117–124.
[28] R. Ikeda, S. Kobayashi, J. Chiba, M. Inouye, Chem. Eur. J. 15 (2009) 4822–4828.